

DEVELOPMENT AND ADJUSTMENT OF "K-ε" TURBULENCE MODEL FOR MHD CHANNEL FLOWS WITH LARGE ASPECT RATIO IN A TRANSVERSE MAGNETIC FIELD

S.Smolentsev and M.Abdou

UCLA, MAE Dept., 44-114 Engineering IV, Los Angeles, CA 90095-1597, USA

T.Kunugi

Kyoto University Dept. of Nuclear Engineering, Yoshida, Sakyo, Kyoto, 606-8501, Japan

1. Introduction

Apart from liquid metals, low-conductivity fluids such as molten salt Flibe ((LiF)_n•(BeF₂)) are being considered as a practical candidate for nuclear fusion applications. For example, a 2 cm thick free surface Flibe layer with a velocity of 10 m/s is used in one of the designs of the APEX study (Advanced Power Extraction) [1]. Unlike liquid metals, Flibe flows do not experience significant MHD forces but remain turbulent because Flibe electrical conductivity is about 30 times greater than that of seawater but 10⁴ times less than that of liquid metals. Under a reactor strong magnetic field, turbulence pulsations in Flibe will be partially suppressed with an accompanying reduction in heat transfer. These effects are under consideration in the present study, where the "K-ε" model of turbulence is adjusted and then applied to the analysis of MHD turbulent flows in closed and open channels with a large aspect ratio under nuclear fusion relevant conditions.

The standard "K-ε" model is widely used in engineering applications. Several studies have been known to extend this model to MHD flows in closed channels in a transverse magnetic field [2-6]. In [2], sink terms standing for the Joule dissipation were added to the equations for "K" and "ε" in the form of

$$C_3 \frac{\sigma}{\rho} B_0^2 K, C_4 \frac{\sigma}{\rho} B_0^2 \varepsilon \quad (1)$$

respectively, with the closure constants $C_3=0.5$ and $C_4=1.0$. In that study, the contribution of the electric field was not taken into account. No applications of the "K-ε" model are known for free surface MHD flows. In more recent studies, special attention has been paid to introduce an anisotropy in the distribution of the turbulent kinetic energy [6], [7] through variations in C_3 and C_4 . In the present study, we focus on the adjustment of the "K-ε" model for channel flows with either a wall-normal or spanwise magnetic field. Also, free surface boundary conditions proposed in [8] for non-conducting liquids have been modified here by taking into account MHD effects.

2. Turbulence model

Assuming low Re_m and applying Reynolds averaging to Navier-Stokes-Maxwell equations with conventional closure approximations, one can derive the following equations for K and ε :

$$\frac{\partial K}{\partial t} + \langle v_j \rangle \frac{\partial K}{\partial x_j} = \underbrace{v_t \left(\frac{\partial v_i}{\partial x_j} \right)^2}_{\text{Production}} + \underbrace{\frac{\partial}{\partial x_j} \left[\left(v + \frac{v_t}{\sigma_K} \right) \frac{\partial K}{\partial x_j} \right]}_{\text{Diffusion}} - \underbrace{\varepsilon - \varepsilon_{em}}_{\text{Dissipation}}; \quad (2)$$

$$\frac{\partial \varepsilon}{\partial t} + \langle v_j \rangle \frac{\partial \varepsilon}{\partial x_j} = C_1 \frac{\varepsilon}{K} v_t \left(\frac{\partial v_i}{\partial x_j} \right)^2 + \frac{\partial}{\partial x_j} \left[\left(v + \frac{v_t}{\sigma_\varepsilon} \right) \frac{\partial \varepsilon}{\partial x_j} \right] - C_2 \frac{\varepsilon}{K} \varepsilon - \frac{\varepsilon}{K} \varepsilon_{em}. \quad (3)$$

The relationship between K , ε , and v_t is given by the conventional Kolmogorov-Prandtl expression: $v_t = C_v K^2 / \varepsilon$. Here, v_t is the eddy viscosity introduced via the Boussinesq approximation, while C_1 , C_2 , C_v , σ_K , and σ_ε are the closure coefficients. The first three terms on the RHS of equation (2) are standard, while the fourth one, ε_{em} , stands for the Joule dissipation. The expression for ε_{em} has been derived here in the most general form as:

$$\begin{aligned} \varepsilon_{em} = & \frac{\sigma}{\rho} [2(B_{01}^2 + B_{02}^2 + B_{03}^2)K - B_{01}^2 \langle v_1^2 \rangle - B_{02}^2 \langle v_2^2 \rangle - B_{03}^2 \langle v_3^2 \rangle - \\ & \underbrace{2B_{01}B_{03} \langle v_1 v_3 \rangle - 2B_{01}B_{02} \langle v_1 v_2 \rangle - 2B_{02}B_{03} \langle v_2 v_3 \rangle}_{D_1} - \\ & \underbrace{B_{01} \left(\left\langle \frac{\partial \varphi}{\partial x_2} v_3 \right\rangle - \left\langle \frac{\partial \varphi}{\partial x_3} v_2 \right\rangle \right) - B_{02} \left(\left\langle \frac{\partial \varphi}{\partial x_3} v_1 \right\rangle - \left\langle \frac{\partial \varphi}{\partial x_1} v_3 \right\rangle \right) - B_{03} \left(\left\langle \frac{\partial \varphi}{\partial x_1} v_2 \right\rangle - \left\langle \frac{\partial \varphi}{\partial x_2} v_1 \right\rangle \right)}_{D_{II}}] . \end{aligned} \quad (4)$$

Formula (4) includes terms with both velocity pulsations (D_I) and electric field fluctuations (D_{II}), which come from two components in Ohm's law: $\sigma \vec{V} \times \vec{B}_0$ and $-\sigma \nabla \varphi$ respectively. In channel flows with a weak transverse magnetic field, the turbulence structure is close to that in ordinary flows where streamwise vortices dominate. For such vortices, the electric potential almost does not vary, and hence $\varepsilon_{em} \approx D_I$. In the case of a strong magnetic field, transition to a 2-D state occurs, in which turbulent eddies are elongated in the field direction, so that $D_{II} \rightarrow D_I$ and $\varepsilon_{em} = 0$ in the limit. This gives ground for modeling ε_{em} using (1) with C_3 and C_4 decreasing from about 2 to 0 as the magnetic field increases. In the present study we use an approximation for C_3 and C_4 similar to that in [6]: $C_3, C_4 \sim e^{-N}$, where $N = Ha^2 / Re$.

3. Equations for channel flows with a large aspect ratio in a transverse magnetic field

We consider electrically isolated straight closed or open channels of a rectangular cross-section, $h \times 2b$, with one of the dimensions much longer than the other ($h \ll 2b$). The magnetic

field is constant and has only one component, applied perpendicular either to the longer side ($B_0=B_y$, Case 1) or to the shorter one ($B_0=B_z$, Case 2). The x-axis coincides with the main flow direction. The flow equations for averaged quantities can be written as follows:

$$\frac{\partial U}{\partial t} + U \frac{\partial U}{\partial x} + V \frac{\partial U}{\partial y} = -\frac{1}{\rho} \frac{\partial P}{\partial x} + f_x + \frac{\partial}{\partial x}[(v + v_t) \frac{\partial U}{\partial x}] + \frac{\partial}{\partial y}[(v + v_t) \frac{\partial U}{\partial y}] + f_{em}; \quad (5)$$

$$\frac{\partial V}{\partial t} + U \frac{\partial V}{\partial x} + V \frac{\partial V}{\partial y} = -\frac{1}{\rho} \frac{\partial P}{\partial y} + f_y + \frac{\partial}{\partial x}[(v + v_t) \frac{\partial V}{\partial x}] + \frac{\partial}{\partial y}[(v + v_t) \frac{\partial V}{\partial y}]; \quad (6)$$

$$\frac{\partial U}{\partial x} + \frac{\partial V}{\partial y} = 0; \quad (7)$$

$$\rho C_p \left(\frac{\partial T}{\partial t} + U \frac{\partial T}{\partial x} + V \frac{\partial T}{\partial y} \right) = \frac{\partial}{\partial x} \left[k \left(1 + \frac{v_t}{v} \frac{Pr}{Pr_{tx}} \right) \frac{\partial T}{\partial x} \right] + \frac{\partial}{\partial y} \left[k \left(1 + \frac{v_t}{v} \frac{Pr}{Pr_{ty}} \right) \frac{\partial T}{\partial y} \right]. \quad (8)$$

In Case 2, the mean electromagnetic force, f_{em} , is negligible because $2b \gg h$. In Case 1, $f_{em} = -\sigma \rho^{-1} B_0^2 (U - h^{-1} \int_0^h U dy)$. The other two forces, f_x and f_y , are related to gravity. For free

surface flows in an inclined chute, $f_x = g \sin \alpha$ and $f_y = -g \cos \alpha$, where α is the inclination angle. To incorporate low-Reynolds number effects the low-Reynolds number modification by Chien [9] was used. The equations were solved using a non-uniform mesh finite-difference method with mapping for tracking the surface. C_3 and C_4 were evaluated by computer optimization using two well-documented experimental sets of friction factor data for isolated slotted channels with a wall-normal [10] and spanwise [11] magnetic field as

$$C_3 = 1.9 \exp(-1.0N); \quad C_4 = 1.9 \exp(-2.0N). \quad (9)$$

4. Free surface boundary conditions

In the first application of the model to ordinary flows, symmetry boundary conditions were used at the surface:

$$\left(\frac{\partial K}{\partial y} \right)_s = 0; \quad \left(\frac{\partial \varepsilon}{\partial y} \right)_s = 0. \quad (10)$$

More accurate free surface boundary conditions were proposed in [8]:

$$\left(\frac{\partial K}{\partial y} \right)_s = 0; \quad \varepsilon_s = \frac{C_v^{3/4} K_s^{3/2}}{0.07 h \kappa}. \quad (11)$$

The second of conditions (11) expresses the experimental fact that the dissipation length scale at the free surface is about 7% of the flow thickness: $l_s=0.07h$. In [8], l was defined as $l = C_v^{3/4} K^{3/2} \epsilon^{-1} \kappa^{-1}$, where κ is the von Karman constant. To incorporate MHD effects we used the following modification of (11). First, two new quantities, l_1 and l_0 , were calculated as the dissipation length scales at the free surface with and without the magnetic field respectively using the symmetry boundary conditions. Then, modified l_s was introduced in (11) in the form of $l_s = 0.07h \times l_1 / l_0$, that results in

$$\left(\frac{\partial K}{\partial y}\right)_s = 0; \quad \epsilon_s = \frac{C_v^{3/4} K_s^{3/2} l_0}{0.07h\kappa l_1}. \quad (12)$$

These boundary conditions work well unless the flow at the surface becomes laminar. For the laminarized surfaces we used (10).

5. Turbulent Prandtl number

In closed channel turbulent flows for liquids like Flibe, the Reynolds Analogy is often assumed, so that $Pr_t \approx 1.0$. However, this is not true for open channel flows near the free surface, because the turbulent transport from the surface is damped due to suppressing the surface-normal turbulent pulsations. Both the geometrical restriction and the gravitation force cause this phenomenon. In terms of the turbulent Prandtl number it means that Pr_{ty} grows as the distance from the surface decreases, while Pr_{tx} does not vary significantly. In the present study, Pr_{ty} was calculated over the near-surface layer by using the eddy diffusivity for momentum obtained on the basis of the "K- ϵ " model, while the eddy diffusivity for heat was taken from experiments for subcritical ($Fr < 1$) water flows [12]. The best fit for Pr_{ty} was found as

$$Pr_{ty} = 0.7[1 + \exp\{37(y/h - 0.89)\}]. \quad (13)$$

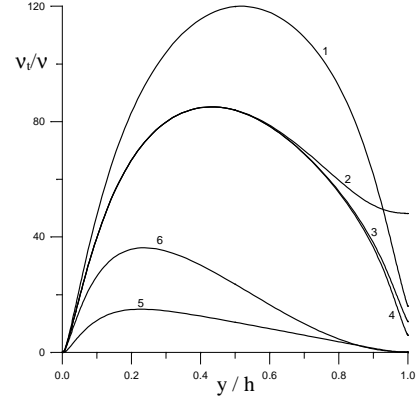


Fig.1. Calculated eddy viscosity with different boundary conditions. $Re=30\,000$, $Fr=0.8$. 1 - $Ha=0$, (11). Case 1: 6 - $Ha=25$, (10). Case 2: 2 - 25, (10); 3 - 25, (11); 4 - 25, (12); 5 - 60, (10).

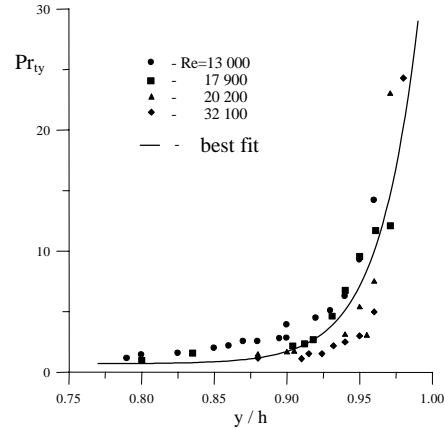


Fig.2. Turbulent Prandtl number near a surface

The best fit for Pr_{ty} was found as

As for Pr_{tx} , the value of 0.7 was used. To our knowledge, the effect of a magnetic field on Pr_{ty} has not been studied. Lacking suitable data for Pr_{ty} , we used (13) in our calculations.

6. Results

The influence of a magnetic field on MHD turbulent flows in closed and open channels is similar. Both the wall-normal and spanwise magnetic field causes the turbulence suppression, which manifests itself through the reduction of the turbulent kinetic energy and the eddy viscosity. However the wall-normal magnetic field leads to a stronger reduction of turbulence due to Hartmann flattening.

The specific features of free surface MHD flows are the effect of a magnetic field on the flow thickness and surface heat transfer reduction. In a spanwise magnetic field, the flow becomes thinner as the field grows. In a wall-normal magnetic field, the thickness decreases first, then it grows at higher Ha due to the Hartmann effect. Fig.3 illustrates the spatial development of the free surface Flibe flow ($U_0=10$ m/s, $h_0=0.023$ m, $\alpha=45^\circ$) over an inclined chute in a spanwise magnetic field. The heat transfer reduction in a fully developed flow ($x > x^*$) is shown in Fig.4. The magnetic field growth leads to a rapid flow laminarization in the near-surface area and as a result the Nusselt number distributions coincide with those in laminar flows if the Hartmann number exceeds a critical value.

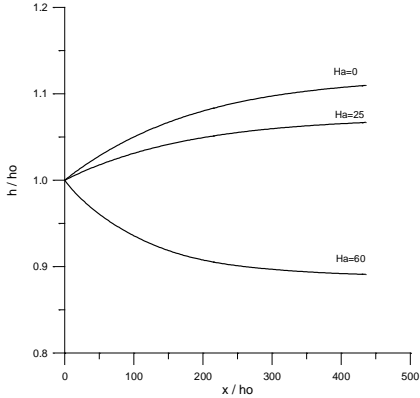


Fig.3. Effect of a spanwise magnetic field on the free surface flow development. $Re=30\ 250$; $Fr=44\ 350$; $\alpha=45^\circ$.

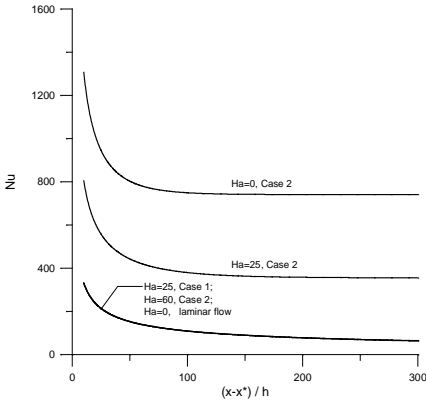


Fig.4. Effect of a magnetic field on surface heat transfer. $Re=30\ 000$; $Fr=0.8$; $Pr=33.8$.

7. Future studies

The model of MHD turbulence and the results presented here reflect a preliminary stage of on-going study. Although expression (1) with the closure coefficients approximated with the exponents gave a reasonable agreement with the experimental data, the model needs further improvements. First, the anisotropy in the turbulence structure associated with the Hartmann effect has not been introduced. As a result, the agreement with experimental data

in Case 1 is slightly worse. Second, the model in its present form gives inaccurate predictions for the case of a streamwise magnetic flux. All these shortcomings send us in search of better modeling for the Joule dissipation term. In our future studies we will pay attention to more accurate modeling of the part of the Joule dissipation term with the electric potential pulsations. Direct numerical simulations will accompany these studies. Also, further evaluation of the turbulent Prandtl number with and without a magnetic field will be conducted based on the FLIHY¹ experimental data for free surface flows in both subcritical ($Fr < 1$) and supercritical ($Fr > 1$) regimes.

We gratefully acknowledge the support provided by the U.S. Department of Energy through contract DE-FG03-88ER52150 A008.

8. Reference

1. M.A.Abdou et al., "Exploring novel high power density concepts for attractive fusion systems," *Fusion Eng. Des.* **45**, 145 (1999).
2. K.Kitamura and M.Hirata, "Turbulent heat and momentum transfer for electrically conducting fluid flowing in two-dimensional channel under transverse magnetic field," in *Proceedings of the 6th International Heat Transfer Conference*, Vol.3, 7-11 Aug. 1978 (Toronto, Canada, 1978), pp.159-164.
3. Yu.Shimomura, "Statistical analysis of magnetohydrodynamic turbulent shear flows at low magnetic Reynolds number," *J. Phys. Soc. of Japan* **57**, 2365 (1988).
4. M.Takahashi, A.Inoue, M.Aritomi, and M.Matsuzaki, "Numerical analysis for laminar and turbulent liquid-metal flow," *Fusion Eng. Des.* **8**, 249 (1989).
5. A.Inoue, Y.Kozawa, M.Takahashi, M.Matsuzaki, and A.Yoshizawa, "Characteristics of flow and heat transfer in air-mercury two-phase stratified flow under a vertical magnetic field," *Exp. Therm. and Fluid Sci.* **8**, 46 (1994).
6. H.-C.Ji and R.A.Gardner, "Numerical analysis of turbulent pipe flow in a transverse magnetic field," *Int. J. Heat Mass Transfer* **40**, 1839 (1997).
7. O.Widlund, S.Zahrai, and F.H.Bark, "Development of a Reynolds stress closure for modeling of homogeneous MHD turbulence," *Phys. of Fluids* **10**, 1987 (1998).
8. H.Ueda, R.Moller, S.Komori, T.Mizushima, "Eddy diffusivity near the free surface of open channel flow", *Int. J. Heat Mass Transfer*, Vol.20, 1127 (1977).
9. K.-Y.Chien, "Predictions of channel and boundary-layer flows with a low-Reynolds number turbulence model," *AIAA J.* **20**, 33 (1982).
10. E.C.Brouillette and P.S.Lykoudis, "Magneto-fluid mechanic channel flow. I. Experiment," *Phys. of Fluids* **10**, 995 (1967).
11. G.G.Branover, A.S.Vasil'ev, Yu.M.Gel'fgat, and E.V.Shcherbinin, "Turbulent flow in a plane perpendicular to a magnetic field," *Magnetohydrodynamics* **4**, 78 (1966).
12. M.S.Hossain, W.Rodi, "Mathematical modeling of vertical mixing in stratified channel flow", *Proc. of the 2nd Symposium on Stratified Flows*, Trondheim, Norway (1980).

¹ FLIHY (FLIbe HYdrodynamics) experimental facilities are pending construction at UCLA